AN ANALYTICAL INVESTIGATION OF THE DUCTED PROPELLER FOR HYDRODYNAMIC PROPULSION

Glenn A. Savage

AN ANALYTICAL INVESTIGATION OF THE DUCTED PROPELLER FOR HYDRODYNAMIC PROPULSION

64

Thesis by

Glenn A. Savage

Lieutenant, United States Navy

In Partial Fulfillment of the Requirements

For the Degree of

Aeronautical Engineer

California Institute of Technology

Pasadena, California

1957

ACKNOWLEDGEMENTS

The author is indebted to Dr. Frank E. Marble for the benefit of frequent discussion, criticism and suggestions which were invaluable during the investigation. The assistance of Miss Ruth Wimmel in typing and assembling the final report is greatly appreciated.

ABSTRACT

An analytical investigation was carried out to determine the design conditions, for a ducted propeller unit operating in water, providing optimum suppression of cavitation when the forward speed, depth and body drag are given. The selection charts were constructed in detail for propellers using the NACA 65 series blades. The results indicate the pumps of generally higher flow rates are more desirable than those that have been employed in the few units actually constructed.

TABLE OF CONTENTS

LIST OF SYMBOLS

A_1	cross-sectional area at entrance to guide vanes (ft^2)
C_D	drag coefficient of propelled vehicle
D	drag (lb)
F	thrust (lb)
K	cavitation number associated with minimum operating depth, at the inception of cavitation
P_a	atmospheric pressure (lbs/ft^2)
P_l	local static pressure (lbs/ft^2)
P_v	vapor pressure of water (lbs/ft^2)
P_T	total pressure (lbs/ft^2)
R	radius of propeller from axis of rotation
S	pressure coefficient across fan blades
S'	propelled vehicle cross-sectional area (ft^2)
W	velocity relative to rotating blade (ft/sec)
c	chord length
d	minimum operating depth (ft salt water)
t	tangential blade spacing (ft)
u	axial velocity, absolute (ft/sec)
v	tangential velocity, absolute (ft/sec)
z	number of blades
α	angle of attack between flow direction and fan blade chord
β	flow angle between flow direction and cascade axis
γ	fan blade stagger angle between cascade axis and blade chord
η_p	propulsive efficiency
θ	turning angle, the difference between flow angle at entrance to fan blade and exit from fan blade

λ drag-area coefficient, propelled vehicle cross-sectional area divided by duct cross-sectional area, times the drag coefficient

π_d diffusion coefficient, absolute axial velocity at inlet to guide vanes divided by free stream velocity

ρ density of sea water (lbs/ft^3)

σ solidity, chord of blades divided by tangential spacing

φ flow coefficient, rotating velocity divided by free stream velocity

ψ turning coefficient, tangential turning velocity divided by free stream velocity

ω angular rotating velocity

Subscripts

0 free stream

1 upstream of guide vanes

2 upstream of rotating fan blades

3 downstream of rotating fan blades

4 downstream of nozzle

I. INTRODUCTION

The ducted propeller is of interest in hydrodynamic applications largely because it offers the possibilities of either high loading at low speeds or cavitation suppression at higher speeds. The present work is concerned primarily with utility of the ducted propeller to suppress cavitation on the propeller blades as a means of achieving reasonably efficient and quiet operation at high speeds. The several actual attempts made to achieve this end have not resulted in marked success largely because the principle was applied to problems where the speed, depth or propeller design were inappropriate. This difficulty is understandable because, at moderate forward speeds, the selection of propeller blading, rotative speed and diffuser design must be made in a rather particular manner to achieve the potential advantage of the ducted propeller. Furthermore there existed no method for selection of the appropriate configuration to satisfy given requirements. It is the purpose of the present analysis to develop a method for finding optimum configurations for suppression of blade cavitation and to carry out design charts in detail for a particular class of propeller blading.

The conceptual model employed is an axial flow ducted fan with guide vanes ahead of the rotating fan blades. Possible physical arrangements are shown in figure 1a, b and c. The flow entering the hydrojet of figure 1a and 1b is that flow from the wake of the vehicle being propelled. The flow entering the hydrojet of figure 1c is the free stream flow. This investigation was limited to considerations of the free stream flow entering the hydrojet. Cavitation was assumed to occur on the fan blade; no consideration was given to the possible

occurrence of cavitation due to the geometry of the diffuser and duct or of the body being propelled. Although it is known that cavitation may occur first at the blade tip or hub, high noise output, loss of efficiency and structural damage are largely associated with cavitation of the blade surface.

In the development of the analysis, the free stream flow velocity u_0 was considered to be ideally diffused to a lower velocity u_1 at the entrance to the guide vanes. The flow through the guide vanes and rotating propeller blades was analyzed using airfoil cascade theory. The flow was treated at a typical radius R from the rotating axis and is thus approximately applicable to any section of the propeller blade. The guide vanes were considered to impart a tangential velocity, v, to the flow entering the rotating blades, the rotating blades were considered to turn the flow back to an axial throughflow, and to increase the total pressure by ΔP_T. It was assumed that the total pressure rise was constant from hub to tip, that the axial flow velocity was constant, and that the radial velocity was negligible. The flow downstream of the rotating fan blades was then discharged through a nozzle to an exit velocity u_4 and an exit pressure P_4, equal to the free stream pressure P_0. Cavitation occurred on the suction side of the rotating blade section when the local static pressure P_ℓ dropped to a certain predetermined value P_v.

The thrust of the unit was determined by elementary application of the momentum theorem to the flow upstream and downstream of the ducted propeller. Since steady motion was assumed, the thrust must

equal the body drag and hence propeller requirements were related to the drag characteristics of the body.

Performance data for the rotor blades was extracted from references (1) and (2) for the NACA 65 series airfoil in cascade. These results were employed to obtain a typical set of selection charts, applicable only to these blades, to illustrate use of the analysis to select appropriate blade sections for a given forward speed, depth of operation and body to be propelled.

II. DEVELOPMENT OF THE ANALYSIS

The thrust of a ducted propeller is derived from the change in momentum of the fluid flow thru the unit. This change in momentum is accomplished by the transfer of energy between the fluid and the rotating propeller blades resulting in a total pressure increase which is converted to kinetic energy in the nozzle. The mass flow thru the duct is described by $\rho u_1 A_1$, where ρ is the density of sea water, u_1 is the absolute axial flow velocity upstream of the guide vanes, and A_1 is the cross-sectional area of fluid flow at the inlet to the guide vanes. By continuity for fluid flow and since ρ is constant for an incompressible fluid, the mass flow upstream and downstream of the hydrojet is also $\rho u_1 A_1$. The change in momentum thru the ducted propeller is therefore the mass flow times the change in velocity between upstream and downstream states, and is equal to the thrust of the hydrojet

$$F = \rho u_1 A_1 (u_4 - u_0) \tag{2.1}$$

This thrust must equal the drag of the unit being propelled in order to maintain a forward speed of u_0. Drag is expressed as

$$D = \tfrac{1}{2} \rho u_0^2 C_D S' \tag{2.2}$$

where C_D is the drag coefficient defined so as to include, in addition to usual aerodynamic drag, the pressure forces over the streamlines separating the flow passing through the pump from that passing around it. S' is the cross-sectional area of the body being propelled. From equations 2.1 and 2.2 we have

$$\frac{u_4}{u_0} = \frac{1}{2}\left(\frac{C_D S'}{A_1}\right)\left(\frac{u_0}{u_1}\right) + 1 \qquad (2.3)$$

Propulsion efficiency is defined as the thrust work divided by the work input and is expressed as

$$\eta_P = \frac{\rho u_1 A_1 (u_4 - u_0) u_0}{\frac{\rho}{2}(u_4^2 - u_0^2) u_1 A_1} \qquad (2.4)$$

which reduces to

$$\eta_P = \frac{1}{\frac{1}{2}\left(\frac{u_4}{u_0} + 1\right)} \qquad (2.5)$$

From equations 2.3 and 2.5 it is seen that two major dimensionless parameters appear that are important to efficiency and to the size requirements of the hydrojet relative to the size of the vehicle. These are defined as

$$\lambda = \frac{C_D S'}{A_1} \quad , \quad \pi_d = \frac{u_1}{u_0} \qquad (2.6)$$

where λ is a combined drag and cross-sectional area coefficient and π_d is a diffusion coefficient from free stream to the guide vanes. The interrelations of λ , π_d and η_P are shown in figure 3.

To analyze the guide vanes and rotating fan, the airfoil cascade theory was applied. An imaginary cylindrical cross-section of the blades is taken with axis coinciding with the axis of rotation. The imaginary cylinder is assumed to have radial extent dR and a radius R

and then is imagined to be unrolled. A row of parallel blade cross-sectional cuts results which extends on to infinity if the pattern is repeated indefinitely. The flow problem then is reduced from a three-dimensional to a two-dimensional problem. The rotational velocity of the rotor blades is represented by a tangential velocity ωR perpendicular to the cascade axis. An observer can assume that he is fixed in a coordinate system relative to the rotating blade sections or in an absolute system with respect to the guide vanes. The difference in the two coordinate system then is only in the rotating velocity, ωR .

The relative spacing of blade sections is described by the solidity, σ , and

$$\sigma = c/t \tag{2.7}$$

where c is the blade section chord length and t is the tangential spacing equivalent to $2\pi R$ divided by the number of blades. The solidity parameter is one of the important design quantities which effects the performance of the airfoil sections and the occurrence of cavitation.

In figure 2 is shown a typical row of guide vanes and rotor blade sections obtained by the unrolling of a cylindrical cross-section. Reference stations are designated as (0) to indicated free stream flow, (1) to indicate the flow entering the guide vanes, (2) as exit from the guide vanes and entrance to the rotating fan, (3) as exit from the rotating fan, and (4) as the exit from the nozzle. The angle between the blade section chord and cascade axis is designated the stagger angle, ζ . The direction of flow relative to the rotating blade sections

is established by the inlet flow angle, β_2, measured from the cascade axis to the direction of flow. Similarly, the exit flow angle β_3, is measured from the cascade axis to the direction of flow relative to and leaving the rotating blades. The difference between the inlet flow angle and the exit flow angle is the turning angle, θ, thru which the flow is turned by the rotating blades.

The flow through the ducted propeller, absolute and relative to the rotating blades, can be represented by a velocity triangle as shown in figure 2. The axial flow velocity was assumed constant therefore $u_1 = u_3$. The flow velocity relative to the rotating fans is obtained by subtracting the rotating velocity, ωR, from the absolute velocity, u_2, entering the blades sections, giving the inlet flow velocity, W_2, relative to the rotating blades. The relative flow velocity leaving the fan is W_3, and is converted to an absolute velocity, u_3, by adding the rotating velocity, ωR, to the relative velocity. The tangential velocity, ν, imparted to the fluid by the rotating blades was assumed to be equal to the tangential velocity imparted by the guide vanes, resulting in the simplified velocity triangles as given in figure 2.

To describe the pressure distribution across the rotating blade section, the pressure coefficient, S, is used as given in references (1) and (2) where

$$S = \frac{P_{2T} - P_2}{\frac{1}{2} \rho W_2^2} \tag{2.8}$$

the total pressure entering the rotating blade section, minus the local

static pressure at any point across the blade section, divided by the inlet dynamic pressure. When the local pressure, P_ℓ , is equal to some predetermined pressure P_v , cavitation is assumed to occur. The value of P_v may be taken as the local vapor pressure of the water or a more suitable figure if knowledge of local conditions permits it. Thus for given inlet conditions there will be a maximum value of the pressure coefficient, S_{MAX} , for operation without cavitation. To relate the free stream conditions to S_{MAX} , a cavitation number K , is employed where

$$K = \frac{P_o - P_v}{\frac{1}{2}\rho u_o^2} \tag{2.9}$$

the free stream static pressure minus the cavitation pressure of sea water, divided by the free stream dynamic pressure. It will be shown that the value of K determines the minimum operating depth d corresponding to P_o for a given operating velocity, u_o . Part of the problem of this analysis is to relate the cavitation number K , to the pressure coefficient, S_{MAX} , where S_{MAX} is known from experimental data.

Two other dimensionless parameters employed for this analysis are the flow coefficient φ , and turning coefficient ψ where

$$\varphi = \frac{\omega R}{u_o} \tag{2.10}$$

$$\psi = \frac{v}{u_o} \tag{2.11}$$

thus relating the rotational velocity and the turning velocity to the free stream conditions.

By the assumption that no losses occur, the total pressure rise, ΔP_T, across the propeller can be obtained by subtracting the free stream total pressure from the exit total pressure so that

$$\Delta P_T = P_{4T} - P_{oT} \tag{2.12}$$

The total pressure is equal to the sum of the static and dynamic pressures so that

$$P_{4T} = P_4 + \tfrac{1}{2} \rho u_4^2 \tag{2.13}$$

and

$$P_{oT} = P_o + \tfrac{1}{2} \rho u_o^2 \tag{2.14}$$

Since the static pressures at entrance and exit are assumed to be equal,

$$\Delta P_T = \tfrac{1}{2} \rho u_o^2 \left[\frac{u_4^2}{u_o^2} - 1 \right] \tag{2.15}$$

However, since no losses occur and the axial flow velocity was assumed constant, we obtain

$$P_{4T} = P_{3T} = P_3 + \tfrac{1}{2} \rho u_3^2 \tag{2.16}$$

$$P_{oT} = P_{1T} = P_1 + \tfrac{1}{2} \rho u_1^2 \tag{2.17}$$

and

$$\Delta P_T = P_3 - P_1 \tag{2.18}$$

Thus, Bernoulli's equation relative to the rotating blades can be applied to obtain the total pressure rise across the hydrojet. Therefore, relative to the rotating blades

$$P_2 + \tfrac{1}{2}\rho W_2^2 = P_3 + \tfrac{1}{2}\rho W_3^2 \tag{2.19}$$

From the velocity triangle of figure 2, it is seen that the relative velocities are

$$W_2^2 = u_1^2 + (v + \omega R)^2 \tag{2.20}$$

$$W_3^2 = u_3^2 + (\omega R)^2 \tag{2.21}$$

where again the axial velocities u_1 and u_3 are equal. Relative to the guide vane, Bernoulli's equation would be

$$P_1 + \tfrac{1}{2}\rho u_1^2 = P_2 + \tfrac{1}{2}\rho u_2^2 \tag{2.22}$$

where

$$u_2^2 = v^2 + u_1^2 \tag{2.23}$$

By combining equations 2.18 thru 2.23 Euler's turbine equation is obtained as follows:

$$\Delta P = P_3 - P_1 = \rho \omega R v \tag{2.24}$$

Therefore from equations 2.15 and 2.24 we obtain

$$\Delta P_T = \rho \omega R \nu = \tfrac{1}{2} \rho u_o^2 \left[\left(\frac{u_4}{u_o} \right)^2 - 1 \right] \tag{2.25}$$

or in terms of the flow coefficient φ and turning coefficient ψ

$$2 \varphi \psi = \left(\frac{u_4}{u_o} \right)^2 - 1 \tag{2.26}$$

When thrust and drag were equated it was found, equation 2.3, that

$$\frac{u_4}{u_o} = \tfrac{1}{2} \frac{\lambda}{\pi_d} + 1 \tag{2.27}$$

Therefore

$$\varphi \psi = \tfrac{1}{2} \frac{\lambda}{\pi_d} \left[\tfrac{1}{4} \frac{\lambda}{\pi_d} + 1 \right] = \tfrac{1}{2} \left(\frac{\lambda}{\pi_d} \right) \left(\frac{1}{\eta_p} \right) \tag{2.28}$$

This important relationship matches the operating characteristics of the ducted propeller, φ and ψ, with the drag of the vehicle being propelled, the relative size of the vehicle and duct cross-section, and the performance of the entrance diffusor. In a sense, the product is a measure of the power requirements of the ducted propeller.

Associated with the rotational speed and turning velocity is the turning angle, Θ, which is the difference in the flow directions at the entrance and exit relative to the rotating blades, therefore

$$\tan \Theta = \frac{\tan \beta_2 - \tan \beta_3}{1 + \tan \beta_2 \tan \beta_3} \tag{2.29}$$

But from the velocity triangle of figure 2 it is seen that

$$\tan\beta_2 = \frac{v + \omega R}{u_1} \tag{2.30}$$

$$\tan\beta_3 = \frac{\omega R}{u_1} \tag{2.31}$$

By substitution and by dividing numerator and denominator of equation 2.29 by the square of the free stream velocity, the turning angle can be determined to be

$$\tan\theta = \frac{\pi_d \psi}{\varphi[\varphi + \psi] + \pi_d^2} \tag{2.32}$$

From equation 2.32 a value of θ can be calculated which then must be matched with experimental performance data for the particular type airfoils being employed for the propeller blades. Associated with this turning angle will be a pressure coefficient, S, which can be allowed to have a maximum value when the local pressure across the blades is equal to the pressure p_v.

From the definition of the pressure coefficient we have that

$$S = \frac{p_{2T} - p_2}{\frac{1}{2}\rho W_2^2} = \frac{p_2 - p_3}{\frac{1}{2}\rho W_2^2} + 1 \tag{2.33}$$

But

$$p_2 = p_0 + \tfrac{1}{2}\rho\left[u_0^2 - (v^2 + u_1^2)\right] \tag{2.34}$$

therefore by dividing numerator and denominator by $\frac{1}{2}\rho u_0^2$ we obtain

$$S = 1 + \frac{\frac{P_o - P_\ell}{\frac{1}{2}\rho u_o^2} + [1 - \pi_d^2 - \psi^2]}{[\varphi + \psi]^2 + \pi_d^2} \qquad (2.35)$$

When the local pressure equals the pressure P_v we have S_{MAX} and since the cavitation number K was defined as

$$K = \frac{P_o - P_v}{\frac{1}{2}\rho u_o^2}$$

we can determine the cavitation number as a function of the ducted propeller performance and operating characteristics

$$K = (S_{MAX} - 1)[(\varphi + \psi)^2 + \pi_d^2] + [\pi_d^2 + \psi^2 - 1] \qquad (2.36)$$

From the definition of the cavitation number it is seen that for a given operating velocity u_o the minimum operating depth d is determined since the free stream static pressure P_o is equivalent to the pressure at the depth d plus the atmospheric pressure. The expression relating K, u_o and d, assuming the vapor pressure of water is zero, is

$$d = \frac{u_o^2}{2g} K - \frac{P_a}{\rho g} \qquad (2.37)$$

and is presented as a nomograph in figure 19. Therefore, from equations 2.36 and 2.37 the operating depth and velocity can be determined as a function of the performance of the rotating blades, the diffusion and power requirements for the ducted propeller. To operate at shallow depths with high velocity it is seen that the pressure coefficient should have a minimum value for the maximum suppression of cavitation.

This in turn requires that the pressure coefficient should have as small a value possible which is equivalent to saying that the velocities across the blade sections must be minimized. Therefore, to suppress cavitation there will be optimum values for all of the dimensionless parameters discussed which will match with the actual performance of the blade sections as given in references (1) and (2) for airfoils in cascade.

In this section, the important relationships have been derived. In the next section the computational procedure carried out to solve the relationships and to match the solutions with the experimental performance data for the 65 series airfoil sections in cascade will be given. A summary of the important relations are as follows:

$$\varphi\psi = \frac{\lambda}{2\pi_d}\left[\frac{\lambda}{4\pi_d} + 1\right] \tag{2.28}$$

$$\eta_p = \frac{1}{\frac{\lambda}{4\pi_d} + 1} \tag{2.5}$$

$$\tan\theta = \frac{\pi_d\psi}{\varphi[\varphi+\psi] + \pi_d^2} \tag{2.32}$$

$$K = (S_{MAX}-1)\left[(\varphi+\psi)^2 + \pi_d^2\right] + \left[\pi_d^2 + \psi^2 - 1\right] \tag{2.36}$$

$$d = \frac{u_o^2}{2g} K - \frac{P_a}{\rho g} \qquad (P_v = 0) \qquad (2.37)$$

III. COMPUTATIONAL PROCEDURE

From equations 2.5 and 2.28 it is seen that for fixed diffusion coefficient π_d and drag-area coefficient λ, the propulsive efficiency η_p, and the product of the flow coefficient φ and turning coefficient ψ are fixed. Then using equation 2.32, the turning angle Θ can be determined for a range of values of φ for a series of constant values of π_d and λ. This was done for values of π_d between .4 and 1.1 and for values of λ between .25 and .75. It was necessary then to match the computed values of the turning angle with the performance data for 65 series airfoils in cascade in order to determine the pressure coefficient, S_{MAX}.

The pressure coefficient S_{MAX} is a function of the solidity, σ, angle of attack, α, stagger angle, ζ, camber and thickness distribution. The data presented in reference (1) gives S and Θ as a function of α for values of solidity equal to .5, .75, 1.00, 1.25 and 1.50, and for values of flow inlet angle, β_2, equal to 30°, 45°, 60° and 70°. The data is also presented for various airfoils of the 65 series with same thickness distributions but different values of camber. In reference (2), data is presented for airfoil sections with the camber reversed in an attempt to reduce velocities across the blade sections.

Fixing the inlet flow angle β_2, and varying the angle of attack α, requires that the stagger angle be varied. However for a fixed blade row the stagger angle must remain fixed requiring that the inlet flow angle vary with the angle of attack. Therefore to use the data

presented in references (1) and (2) it was necessary to cross plot the data to obtain data for fixed airfoil geometry. The cross plotting was carried out for stagger angles of 45° and 55°. Figure 5 is an example of the results for the 65 410 airfoil in cascade with a solidity of 1.0, stagger angle 55°, and with S_{MAX} and θ plotted vs α.

The computed values of turning angle, θ, were then entered into the cross plots to determine the maximum value of the pressure coefficient, S_{MAX}, corresponding to the values of π_d, λ, φ and ψ. Having S_{MAX}, the cavitation number K was calculated and plotted. Figure 10 shows an example of such a plot for $\lambda = .5$, $\vartheta = 55^{\circ}$, $\sigma = 1.0$ where the curves represent values of K and φ for fixed values of π_d. A cross plot was then made for constant values of the cavitation number K as a function of π_d and φ. Figure 13 is an example of the contour plots of K obtained and since a minimum value of K is required for the maximum suppression of cavitation the design point for the given conditions is the center of the contour representing the minimum value of the cavitation number.

IV. DISCUSSION OF ANALYTICAL RESULTS

To determine the effect of the solidity, three cavitation number contour plots were made for values of σ = 1.0, 1.25 and 1.50 where the stagger angle was fixed at 55° and $\lambda = \frac{C_0 S'}{A_1}$ was fixed at .5 . Figures 13, 15 and 16 are the result and clearly show that solidity should have a value of approximately 1.25. Similar plots for values of σ equal to .75 and .5 were not made because by inspection of the S_{MAX} and Θ vs α plots (not shown) the values of S_{MAX} are somewhat higher than for the values shown in figures 5, 6 and 7.

The effect of stagger angle, which is another important design parameter, can be determined by inspection of S_{max} and Θ plots. The values of S_{MAX} for stagger angles less than 45° are larger near design point (minimum S_{MAX}) but will give a larger spread of values of φ for minimum values of K . For stagger angles greater than 55° the values of S_{MAX} are again larger and also the spread of values of φ is more limited. In figures 11 and 13 a comparison for stagger angles of 45° and 55° can be made with all other conditions remaining fixed. The increase to stagger angle, ζ , from 45° to 55° has shifted the design point slightly to the right, decreased the minimum value of the cavitation number, and increased the area inclosed by values of constant K . Any further increase to the stagger angle can be expected to shift the design further to the right and increase the minimum values for K . The physical significance of shifting the design point to the right is that larger values of φ can be employed which means that the rotational velocity can be increased for a given value of u_0 , and

that the loading of the blades is decreased by a decrease in the angle of attack. The optimum value for the stagger angle appears to be approximately 55° for the airfoils considered.

The effect of drag-area coefficient, λ , is quite pronounced in shifting the design point. Calculations were made and plotted for values of λ = .25, .50 and .75 . The value of λ = 0.25 is generally appropriate for a good torpedo shape. The resulting cavitation number contour plots are shown in figures 12, 13 and 14. In addition, constant values of K are cross plotted to figure 3 to show the effect of λ on K as well as propulsive efficiency, η_p . From the figures it is seen that increasing λ shifts the design point to the right, increasing φ , and up, increasing the design value for the diffusion coefficient π_d . It also radically increases the minimum values of K that can be obtained, thus restricting the operating velocity and minimum depth of operation. Therefore, for the maximum suppression of cavitation, the drag-area coefficient, λ , should be as small as possible. This requires a small value at the drag coefficient, C_D , and a small value for the ratio of cross-sectional area of unit being propelled to the cross-section area of the duct. If the drag at the unit is high, a comparatively large ducted propeller will be required. The value of λ therefore has a marked effect in determining the maximum size of a vehicle for propulsion by ducted propeller.

To reduce the problem of obtaining diffusion ratios other than 1.0, a maximum value of λ is desirable since the design value of π_d increases with λ . In order to obtain a larger range of values for

the flow coefficient φ figures 12 through 14 indicate that a minimum value for λ is required. Since $\varphi \sim R$ for given speed and angular velocity, large range in φ is desirable to permit a large hub ratio and hence a small outer diameter. From figure 3 it is evident that decreasing λ will increase the propulsive efficiency η_p. In view of the above considerations, a low value for λ is again more desirable than a high one.

The effect of increase in camber of the blade sections is to increase the velocities across the blade surfaces and thus increase the pressure coefficient, $S_{MAX.}$ Calculations and plots were made for the 65-410 and 65-810 airfoil sections for comparison where stagger angle and λ were fixed. The results are shown in figures 13 and 17 and show that increase in camber from 4 °/o to 8 °/o shifts the design to the left, decreasing the design value for φ. The minimum value for the cavitation number, K, has not been appreciably affected but the areas enclosed by constant values of K have been reduced considerably, reducing the range of φ values available for a given design value for K. The plots of S_{MAX} and θ vs α for airfoil sections with greater cambers show that S_{MAX} increases considerably and that the range of useful values of φ will be reduced further.

In figure 18, the resulting contour plot for the 65-$(8A_2\ I_{8b})$10 airfoil sections is shown to point out the effect of reversing the camber distribution to reduce local velocity ratios. Although this decreases the minimum value of K, the range of values for φ at fixed π_d, is decreased severely. Thus it does not appear advantageous to reduce

local velocities over blade surface by this technique.

To illustrate how data given in the figures can be employed to determine optimum design conditions for the maximum suppression of cavitation, assume that a unit is to be propelled at a velocity of 75 ft/sec (45 knots) and is to operate at a depth of ten feet. From the previous discussion it was seen that a minimum value of the drag-area coefficient is required. Therefore, design considerations for the unit will be for as low a drag coefficient, C_D , as possible, and for as favorable a cross-sectional area ratio as possible consistant with size, weight and space available to the unit being propelled. Assume that the best value of λ that can be obtained is 0.5 . From figure 19 it is found that the maximum allowable value for the cavitation number is approximately 0.5 . For any value greater than 0.5, cavitation can be expected to occur. For λ = 0.5, figure 15 for the 65-410 blade section appears to have the largest area enclosed by a cavitation number of 0.5 . It gives a large range for the values of φ and requires a diffusion coefficient, π_d , of 0.61 . The solidity and stagger angle in this case are 1.25 and 55° respectively. The center of the contour representing the minimum values of K would be designated as the design point for the mean radius R between hub and tip. This value for φ = 1.15 then would fix the optimum angular velocity ω and thus fixes the values for φ for changes in radius R from hub to tip. The ratio of the maximum and minimum flow coefficient contained within the boundaries for K = 0.5 and π_d = 0.61 is approximately 1.3 . This indicates that a relatively large size hub will be necessary, the actual

size being fixed by the value of cross-sectional area decided upon in fixing λ .

From figure 3, the propulsion efficiency can be determined. Then from the propulsive efficiency and drag coefficient, the power requirements can be determined by replacing the thrust work by drag and solving for work input in equation 2.4. Thus a design criterion has been established for the maximum suppression of cavitation.

If optimum diffusion coefficient values could not be obtained, if greater velocities were required, or if the value of the drag-area coefficient λ were unfavorable, it would be necessary to increase the minimum depth of operation and hence raise the free stream pressure P_o .

V. CONCLUDING REMARKS

An attempt has been made to determine what design and operating criteria are necessary to select a ducted propeller propulsion unit with the maximum suppression of cavitation. The detailed selection charts were limited to the NACA 65-series airfoils for propeller blades. The technique, however, is general.

The most sensitive parameter appears to be the drag-area coefficient, λ . This quantity should have as low a value as possible in order to increase the range of propeller operation without cavitation. The diffusion coefficient Π_d is also a significant parameter and it is an interesting result that an optimum retardation of the stream exists; the stream may be slowed down too much as well as too little.

The flow coefficient parameter, φ , was found to have a rather low optimum value, requiring relatively slow rotating velocities or through flow velocities much larger than conventional. In addition it was found that the range of values for φ without cavitation will be somewhat limited. The design criteria for φ are largely determined by the blade sections being employed for the propeller, requiring low velocities across the blades with high loading of the blades.

For the blade sections investigated, it is found that there are optimum values for the solidity σ , the stagger angle, ζ , and the camber. The optimum values are those that will provide minimum values of the maximum pressure coefficient, S_{MAX} , over as large a range of angles of attack as possible, and with limit on the maximum values of the turning angle.

REFERENCES

1. Herrig, L. J., Emery, J. C. and Erwin, J. R., "Systematic Two-Dimensional Cascade Tests of NACA 65-Series Compressor Blades at Low Speeds", NACA RM L51G31 (September 1951).

2. Erwin, J. R., Savage, M. and Emery, J. C., "Two-Dimensional Cascade Investigation of NACA Compressor Blade Sections Having a Systematic Variation in Mean-Line Loading", NACA TN 3817 (November 1956).

3. Keller, C., The Theory and Performance of Axial Flow Fans, McGraw-Hill Book Co., Inc., (1937).

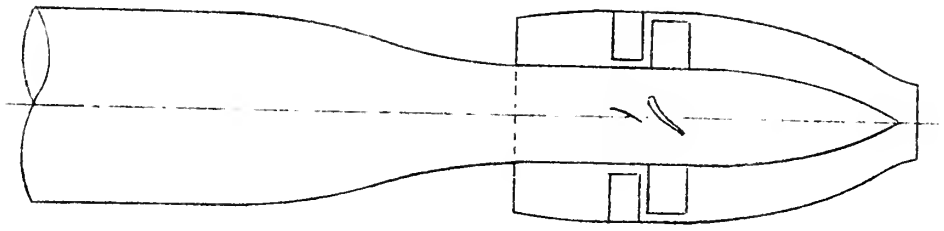

a) Wake flow entering hydrojet .

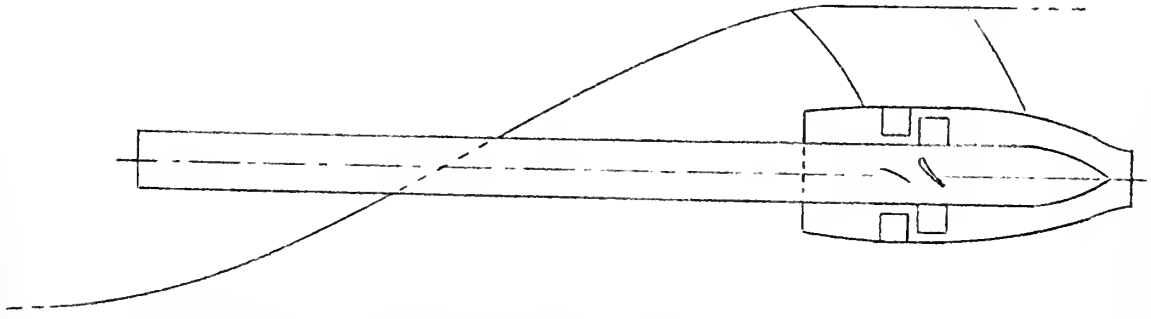

b) Wake flow entering hydrojet driven by conventional propeller shaft .

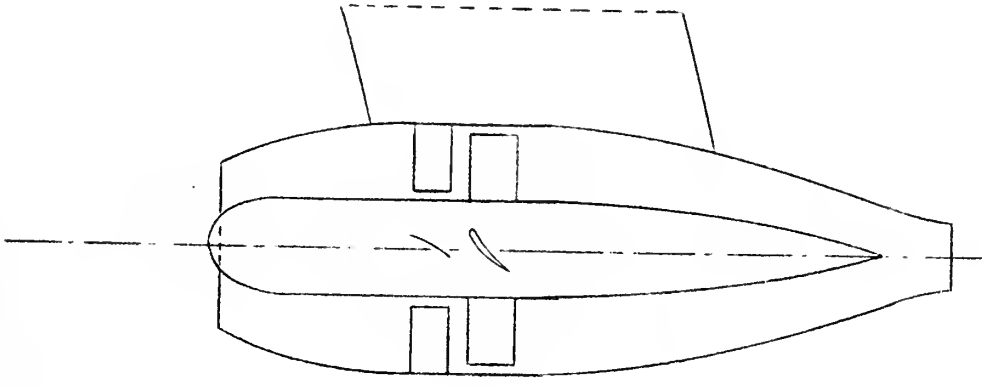

c) Free stream flow entering hydrojet

Figure 1. Schematic of possible hydrojet propulsion configurations.

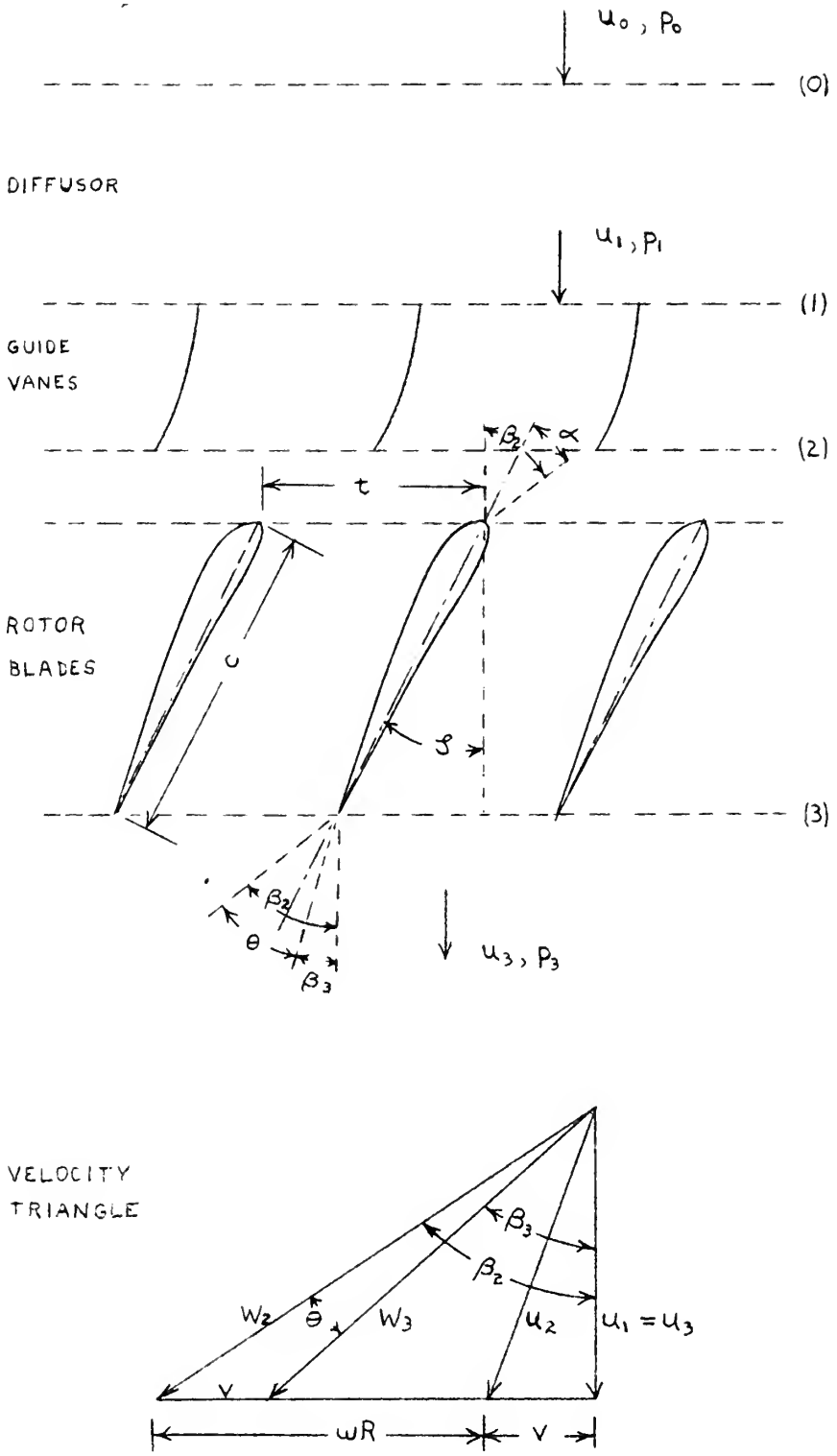

Figure 2. Schematic of guide vanes and hydrojet blade sections in cascade and the associated velocity triangle.

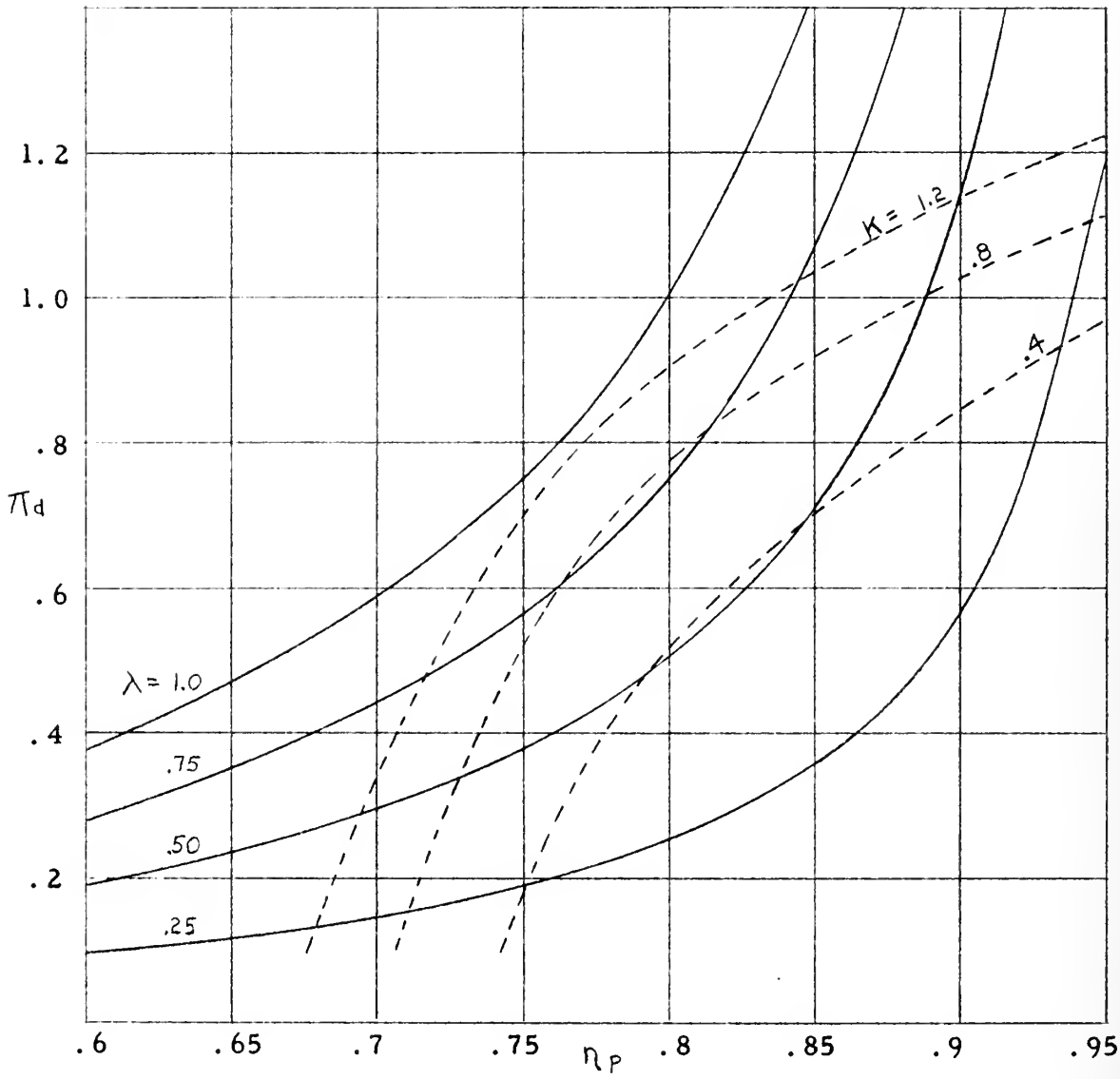

Figure 3. Diffusion coefficient, Π_d, versus propulsion efficiency η_p, for constant drag-area coefficient, λ. Constant values of K are shown for the combination $\sigma = 1.25$, $\mathcal{S} = 55^\circ$ and NACA 65-410 blade section.

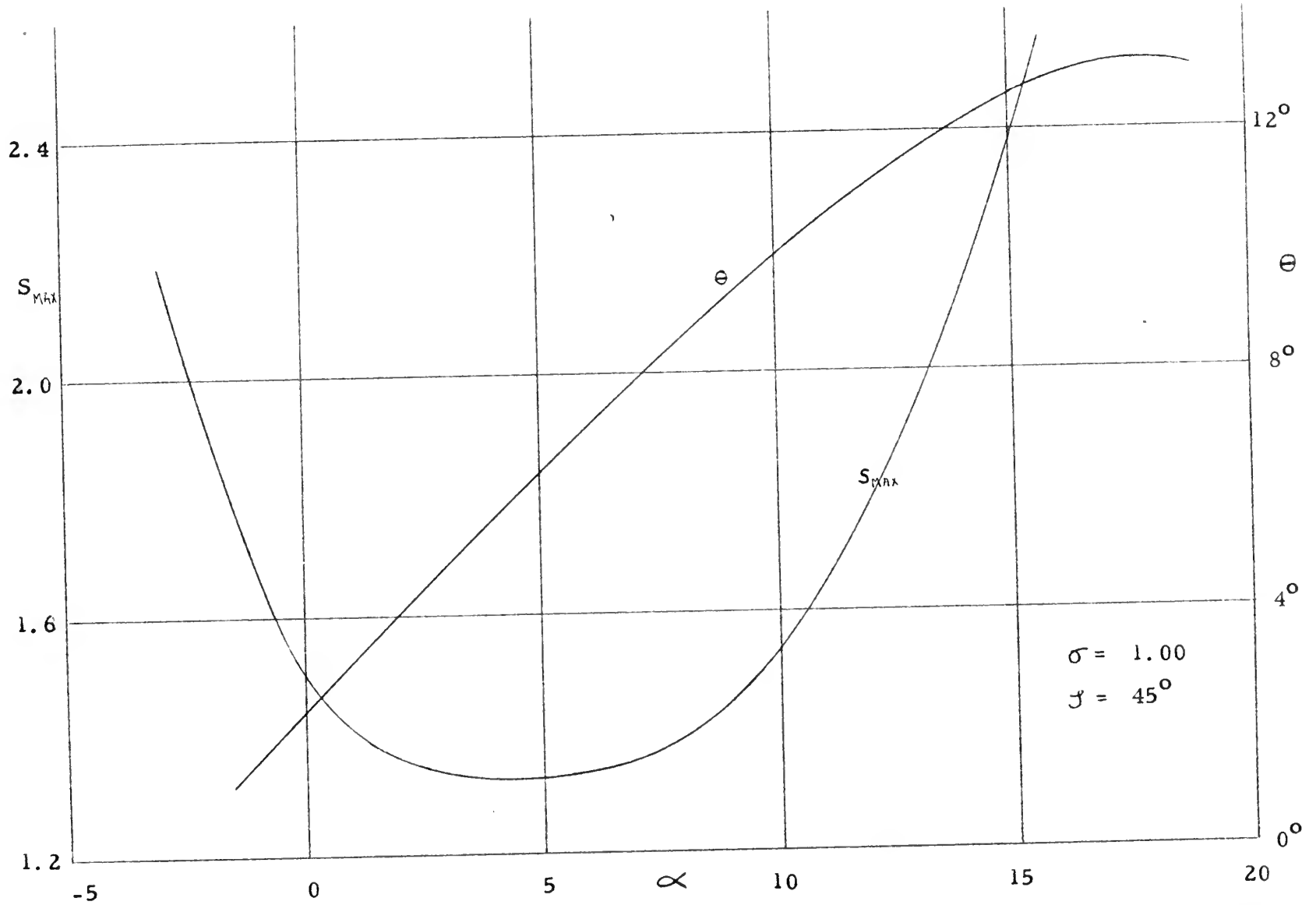

Figure 4. Maximum pressure coefficient S_{MAX} and turning angle Θ for the cascade combination $\sigma = 1.0$, $\gamma = 45^{\circ}$ and NACA 65-410 blade section.

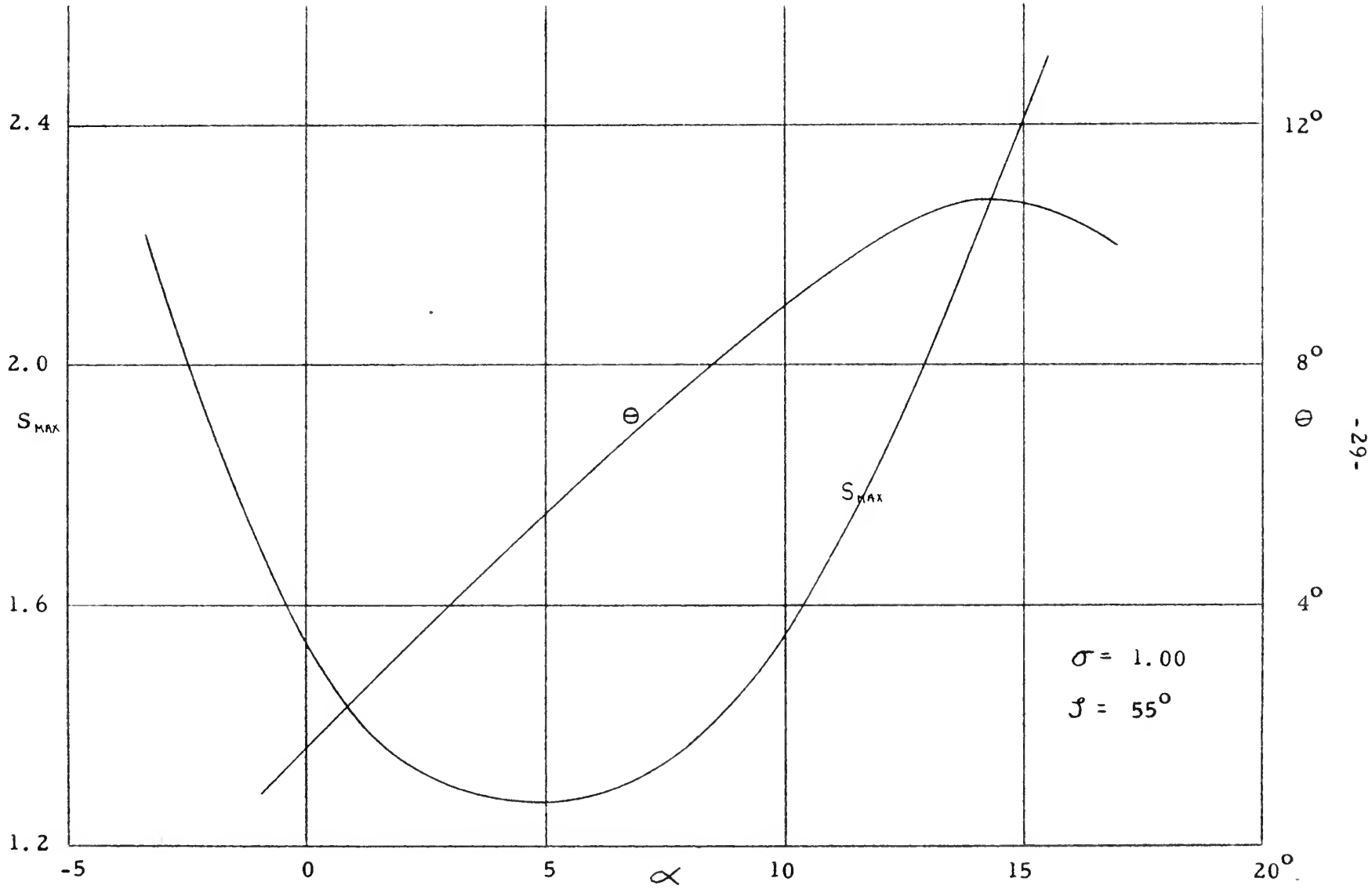

Figure 5. Maximum pressure coefficient S_{MAX} and turning angle Θ for the cascade combination $\sigma = 1.0$, $\vartheta = 55^{\circ}$ and NACA 65-410 blade section.

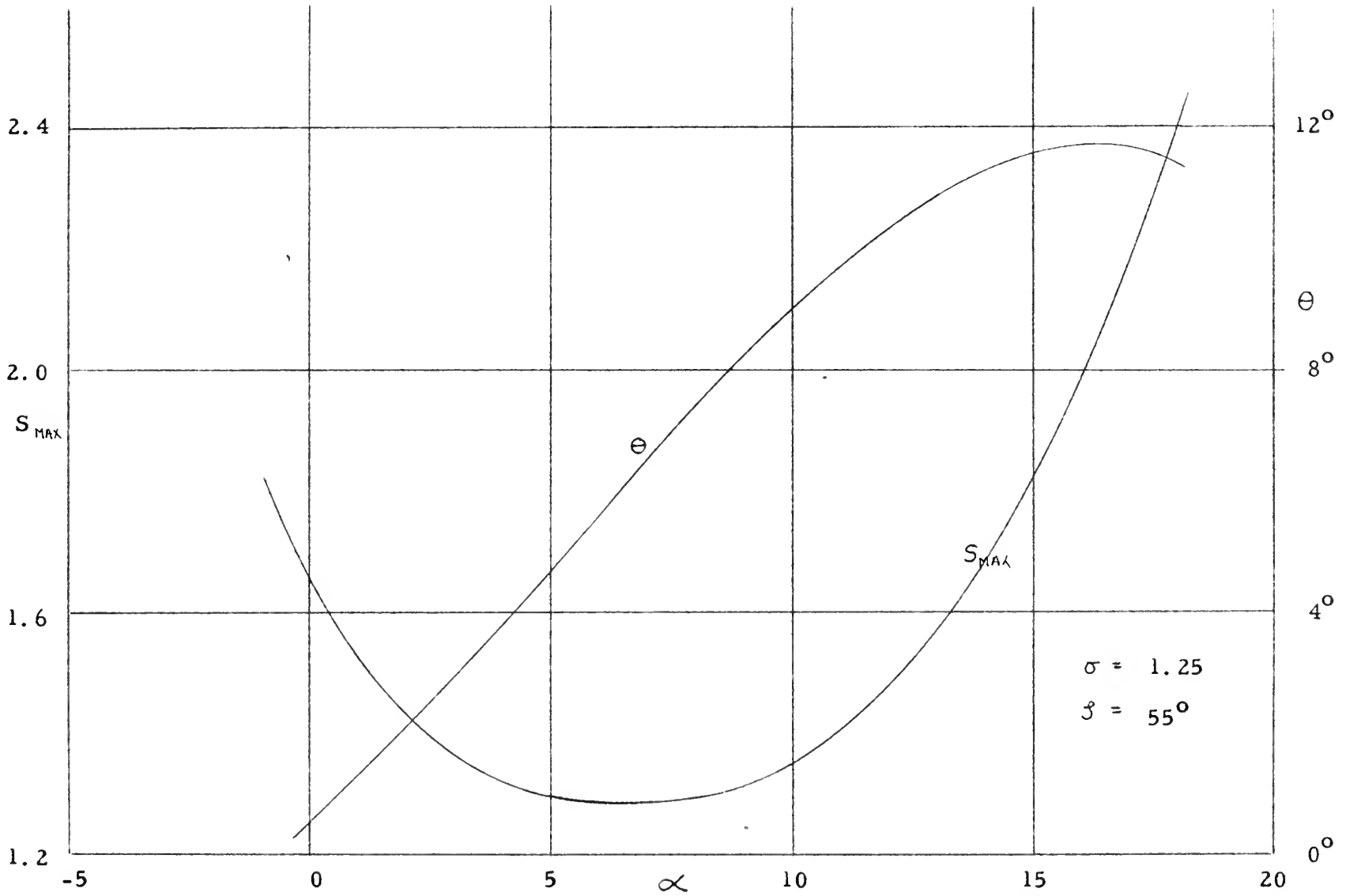

Figure 6. Maximum pressure coefficient S_{MAX} and turning angle Θ for the cascade combination $\sigma = 1.25$, $\vartheta = 55^{\circ}$ and NACA 65-410 blade section.

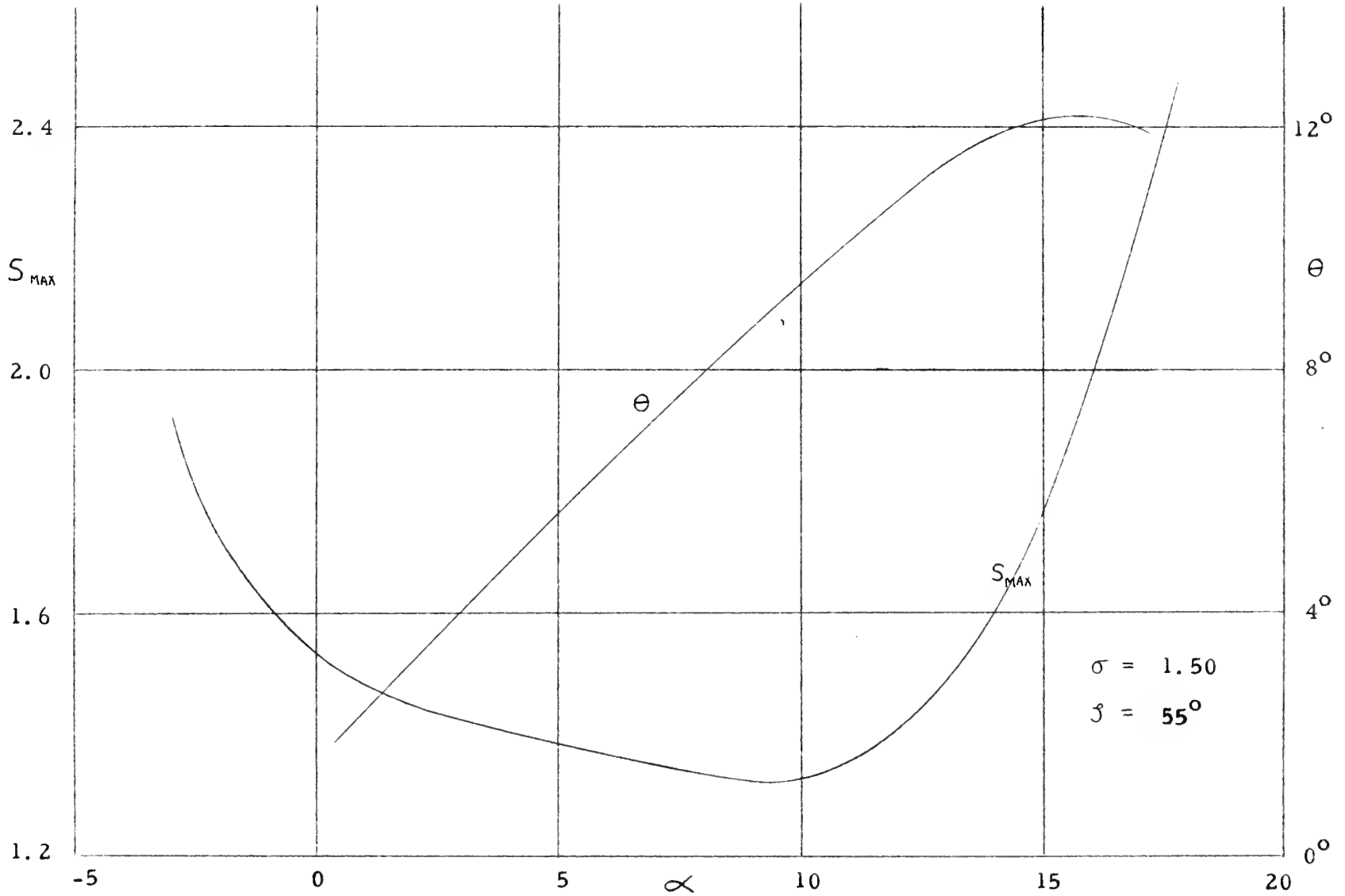

Figure 7. Maximum pressure coefficient S_{MAX} and turning angle θ for the cascade combination $\sigma = 1.5$, $\vartheta = 55^{\circ}$ and NACA 65-410 blade section.

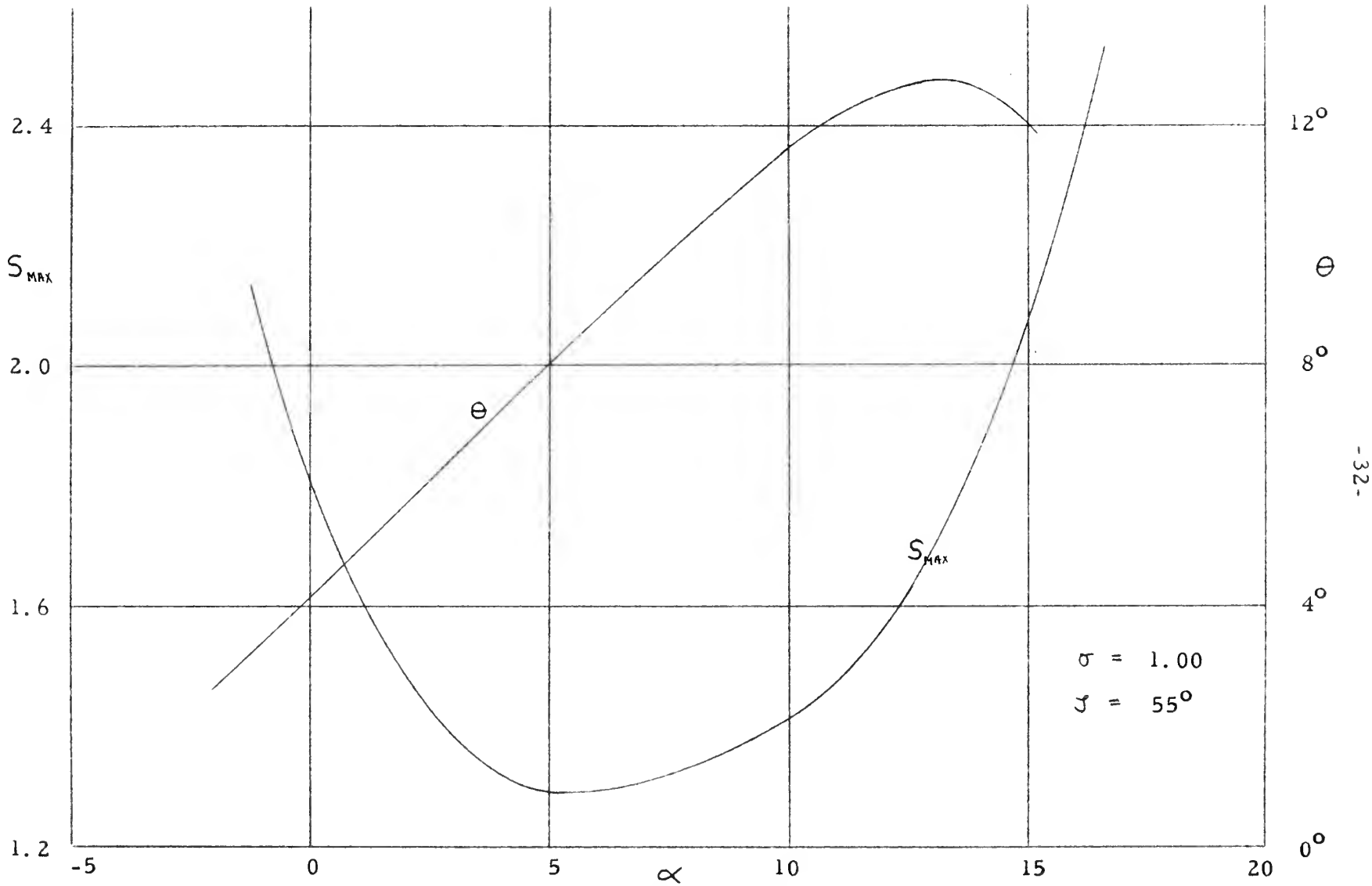

Figure 8. Maximum pressure coefficient S_{MAX} and turning angle Θ for the cascade combination $\sigma = 1.00$, $\gamma = 55^{\circ}$ and NACA 65-810 blade section.

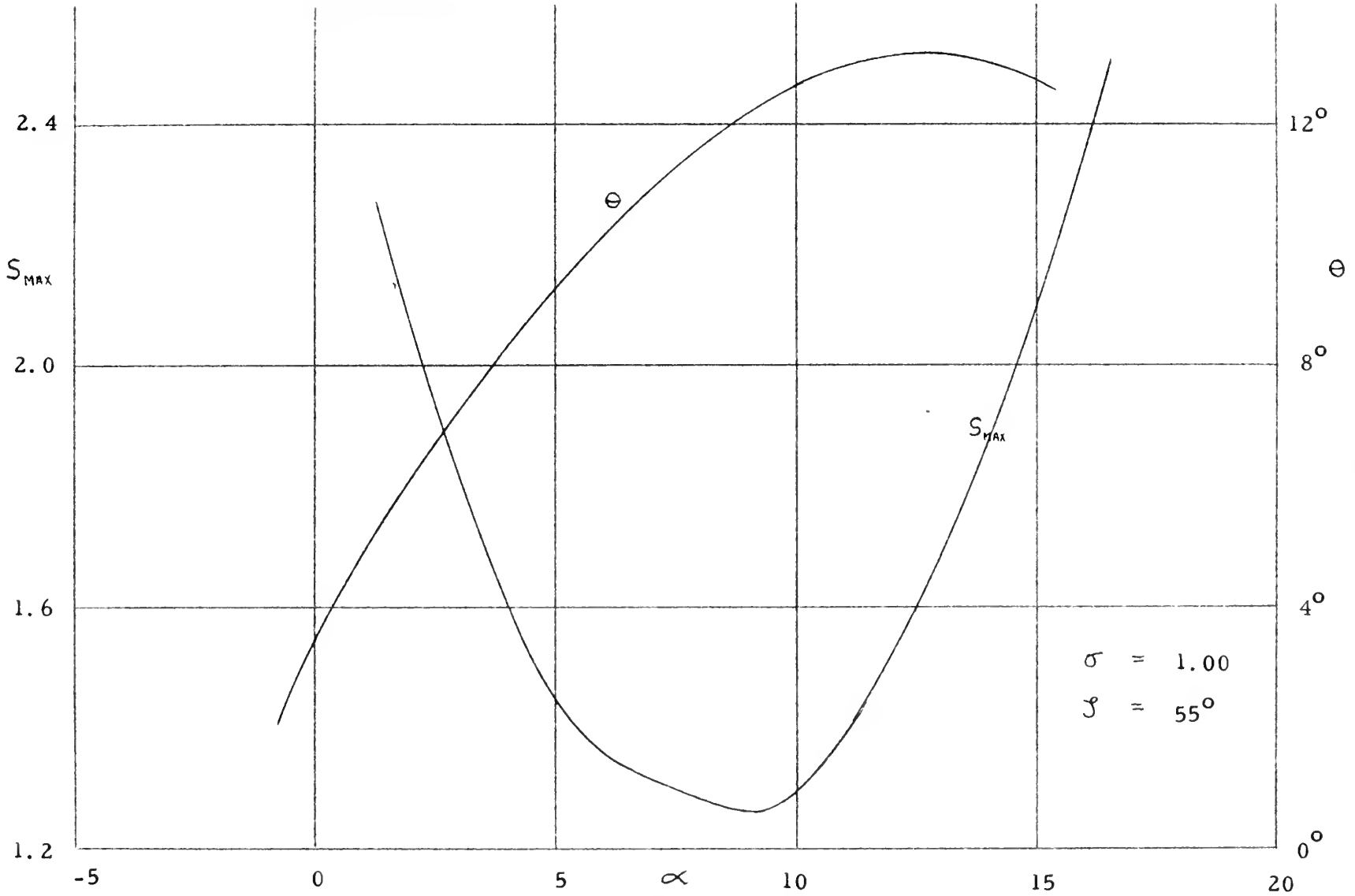

Figure 9. Maximum pressure coefficient S_{MAX} and turning angle Θ for the cascade combination $\sigma = 1.0$, $\vartheta = 55^{\circ}$ and NACA 65-$(8A_2\ I_{8b})10$ blade section.

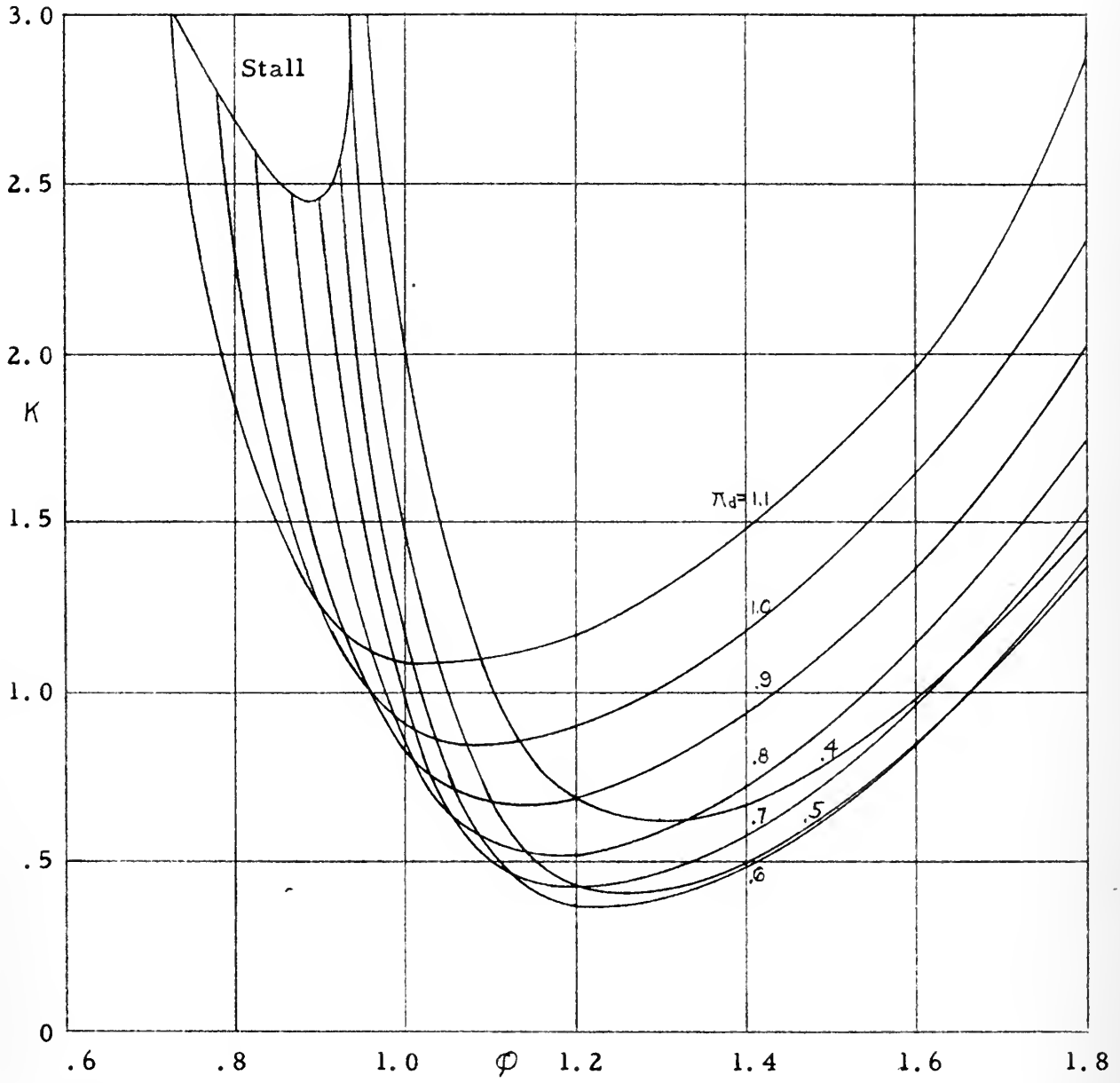

Figure 10. Cavitation number K vs. flow coefficient φ for constant diffusion coefficient π_d for the cascade combination $\sigma = 1.0$, $\gamma = 55^\circ$, $\lambda = .5$ and NACA 65-410 blade section.

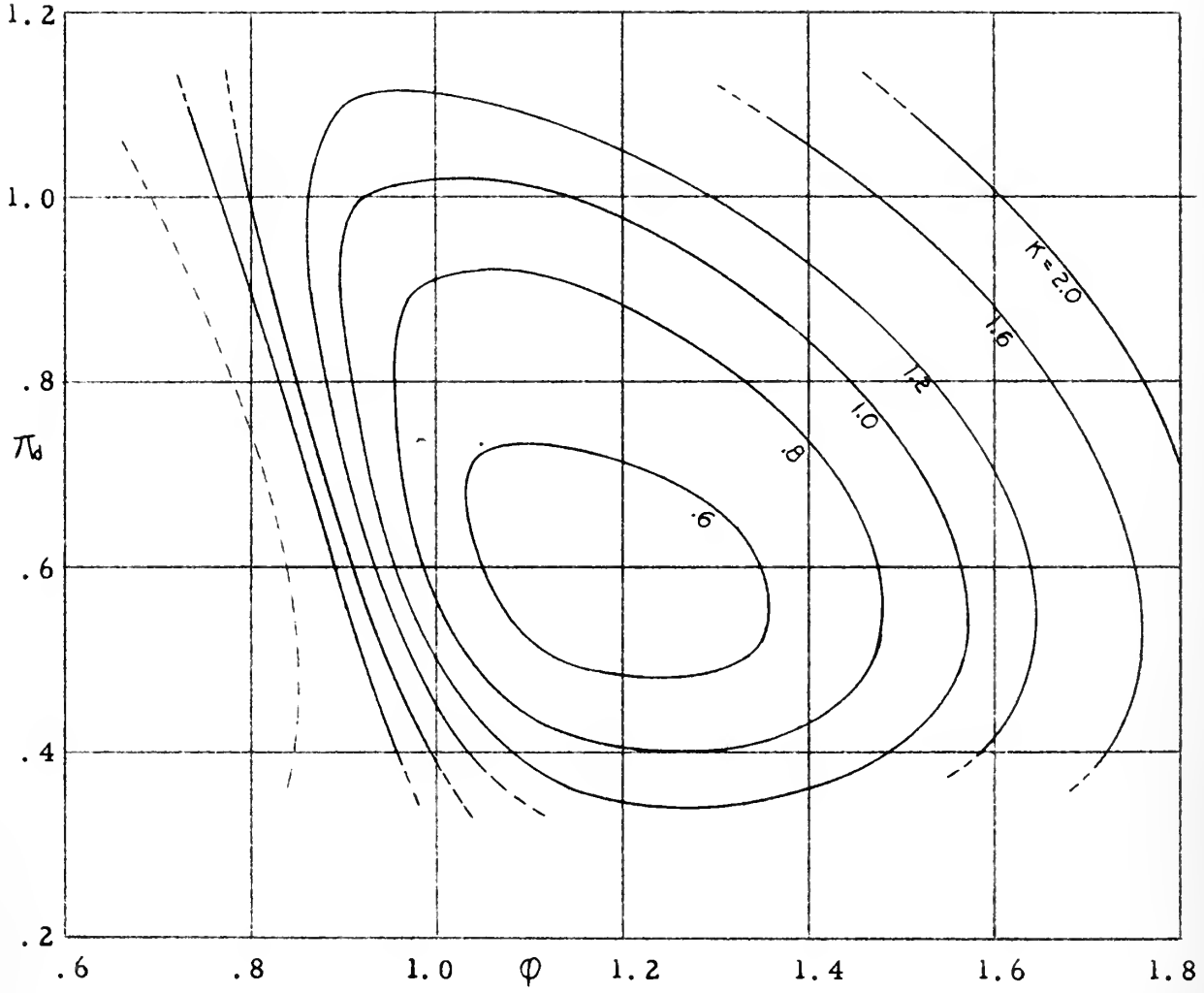

Figure 11. Diffusion coefficient π_d vs. flow coefficient φ for constant values of cavitation number K for the combination $\lambda = .5$, $\sigma = 1.00$, $\beta = 45^\circ$ and NACA 65-410 blade section.

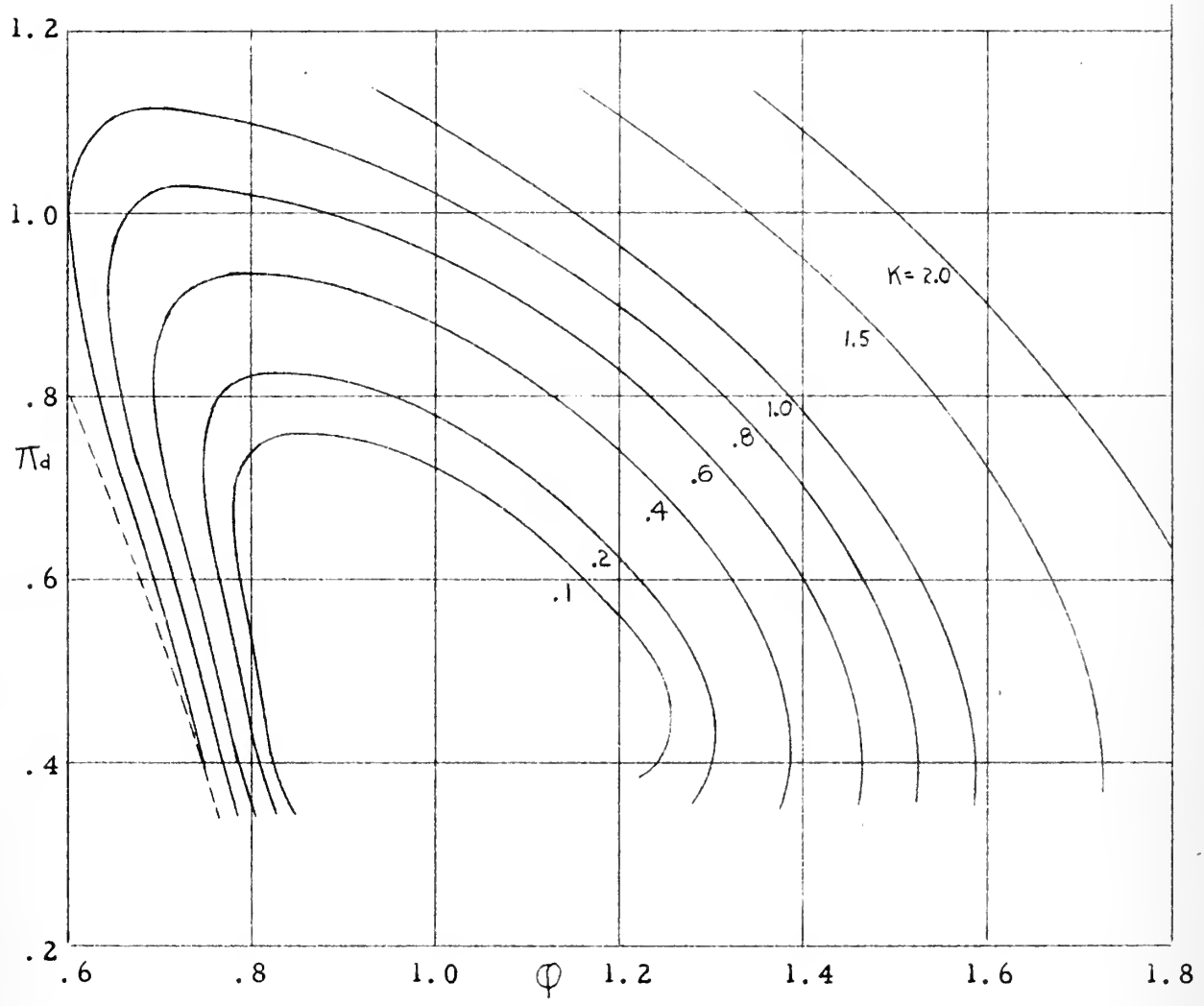

Figure 12. Diffusion coefficient Π_d vs flow coefficient φ for constant values of cavitation number K for the combination $\lambda = .25$, $\sigma = 1.0$, $\beta = 55^\circ$ and NACA 65-410 blade section.

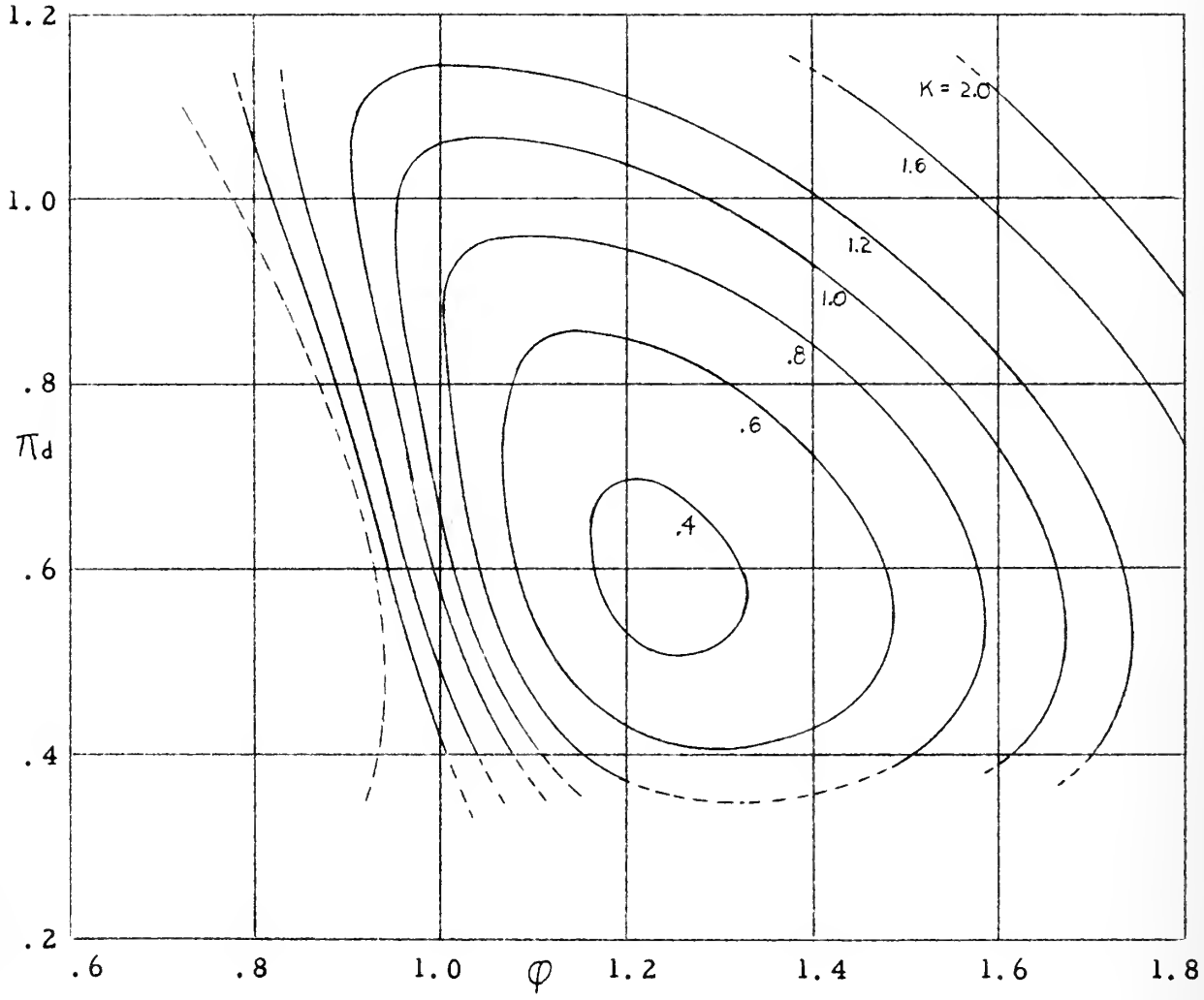

Figure 13. Diffusion coefficient π_d vs flow coefficient φ for constant values of cavitation number K for the combination $\lambda = .5$, $\sigma = 1.00$, $\mathcal{S} = 55^\circ$ and NACA 65-410 blade section.

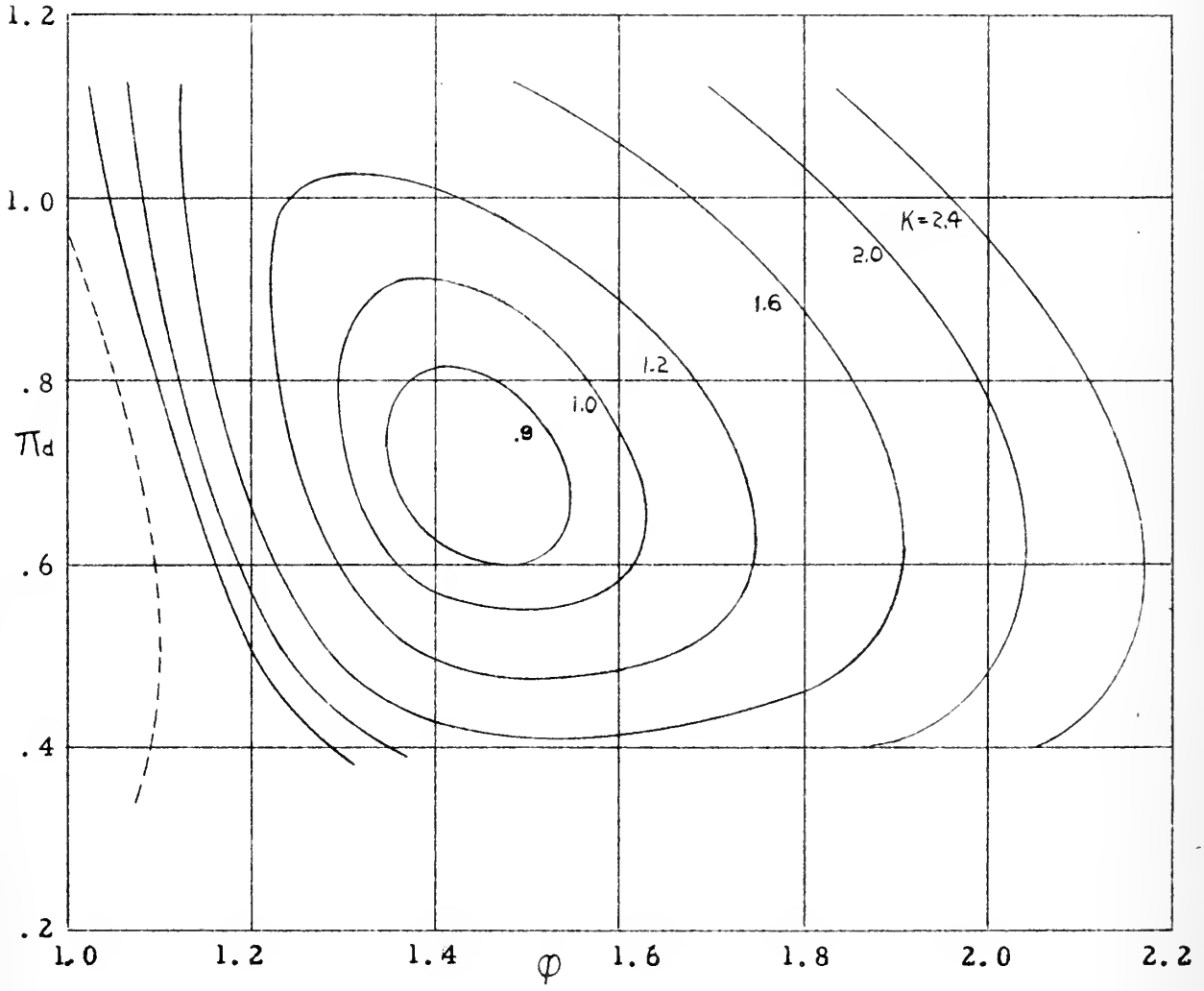

Figure 14. Diffusion coefficient Π_d vs flow coefficient φ at constant values of cavitation number K for the combination $\lambda = .75$, $\sigma = 1.00$, $\beta = 55^\circ$ and NACA 65-410 blade section.

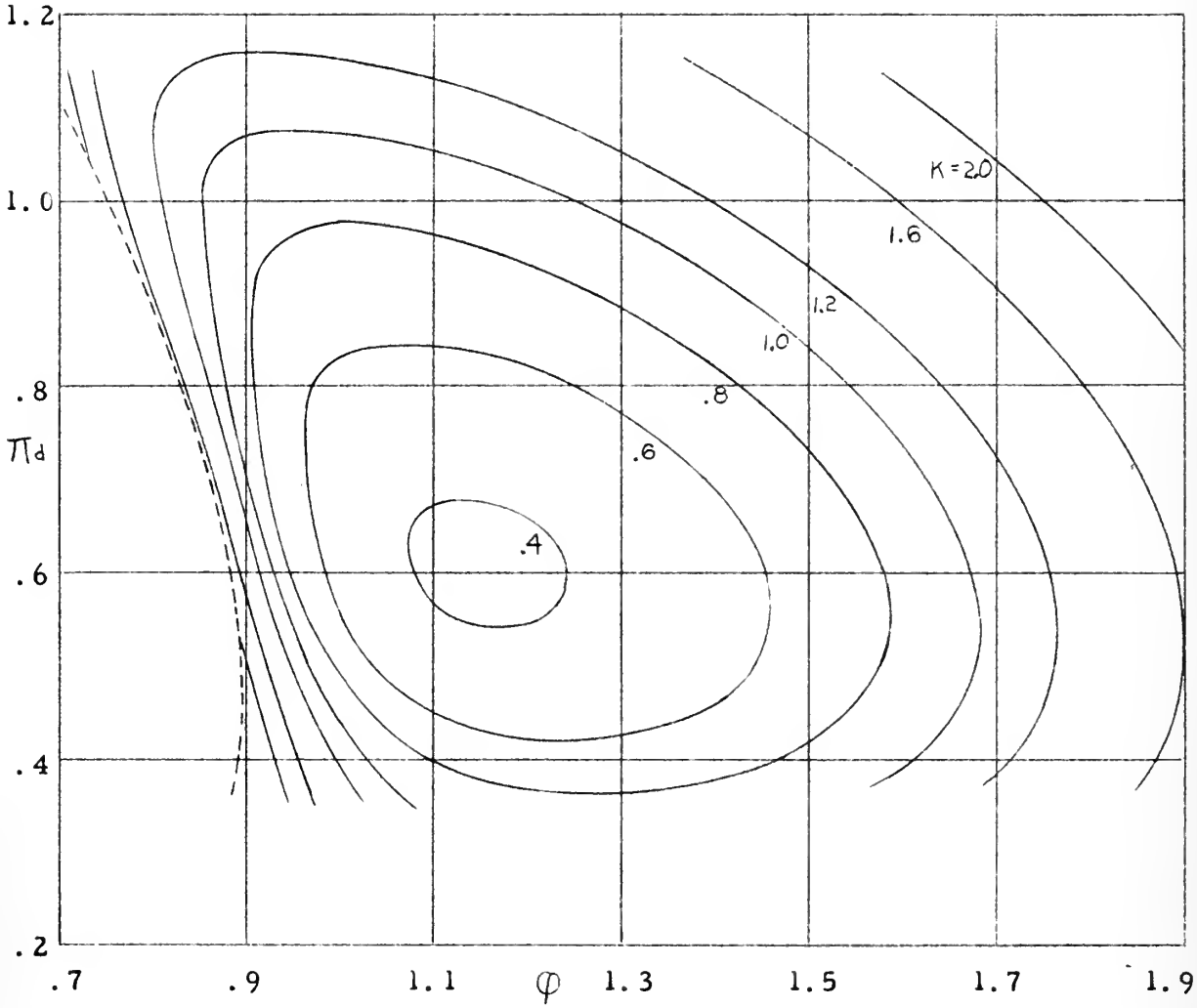

Figure 15. Diffusion coefficient Π_d vs flow coefficient φ for constant values of cavitation number K for the combination $\lambda = .5$, $\sigma = 1.25$, $\mathcal{J} = 55^{\circ}$ and NACA 65-410 blade section.

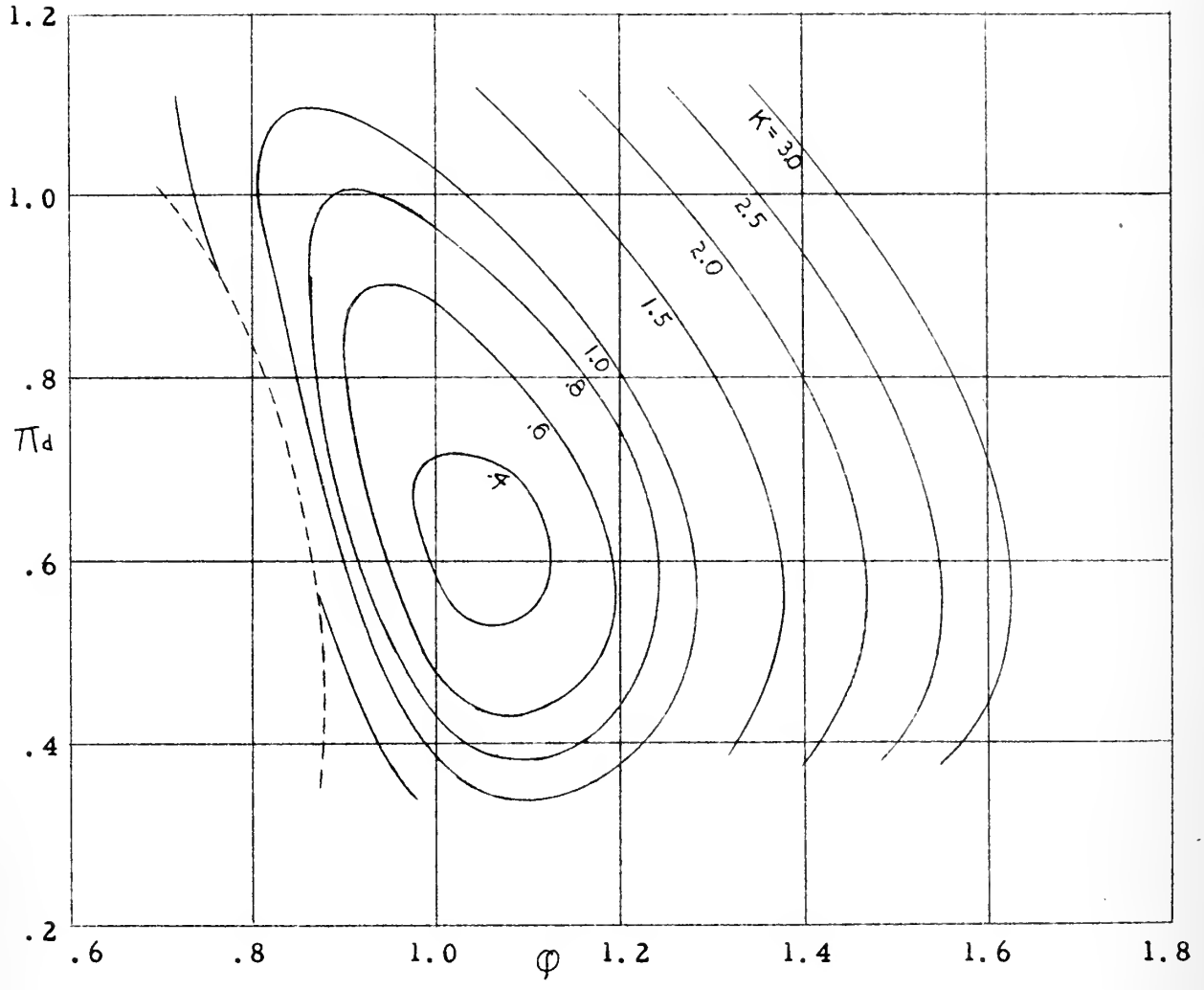

Figure 16. Diffusion coefficient π_d vs flow coefficient φ for constant values of cavitation number K for the combination $\lambda = .5$, $\sigma = 1.5$, $\vartheta = 55^\circ$ and NACA 65-410 blade section.

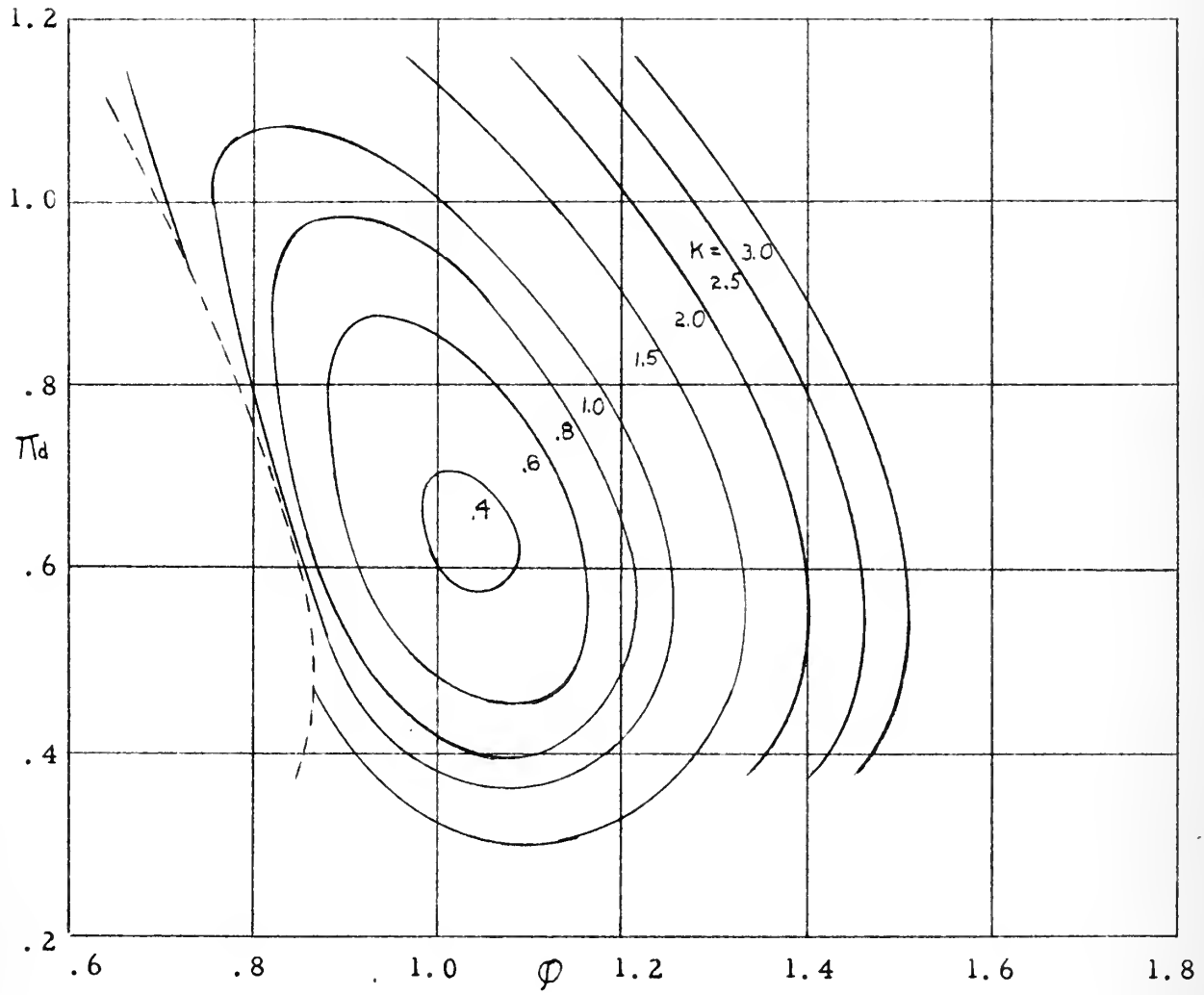

Figure 17. Diffusion coefficient π_d vs flow coefficient φ for constant values of cavitation number K for the combination $\lambda = .5$, $\sigma = 1.00$, $\beta = 55^\circ$ and NACA blade section 65-810.

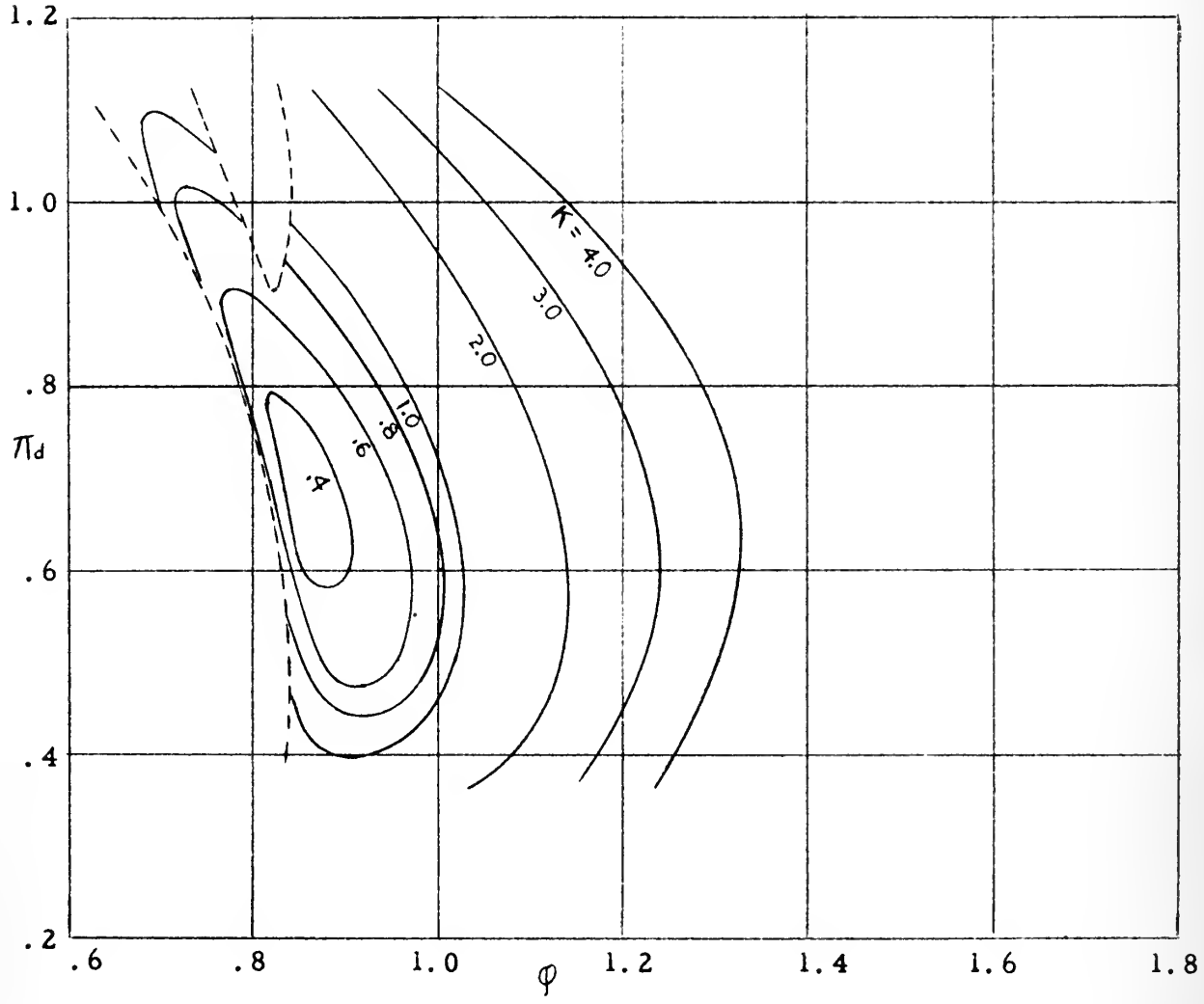

Figure 18. Diffusion coefficient π_d vs flow coefficient φ for constant values of cavitation number K for the combination $\lambda = .5$, $\sigma = 1.00$, $\mathcal{J} = 55^{\circ}$ and NACA 65-$(8A_2\ I_{8b})10$ blade section.

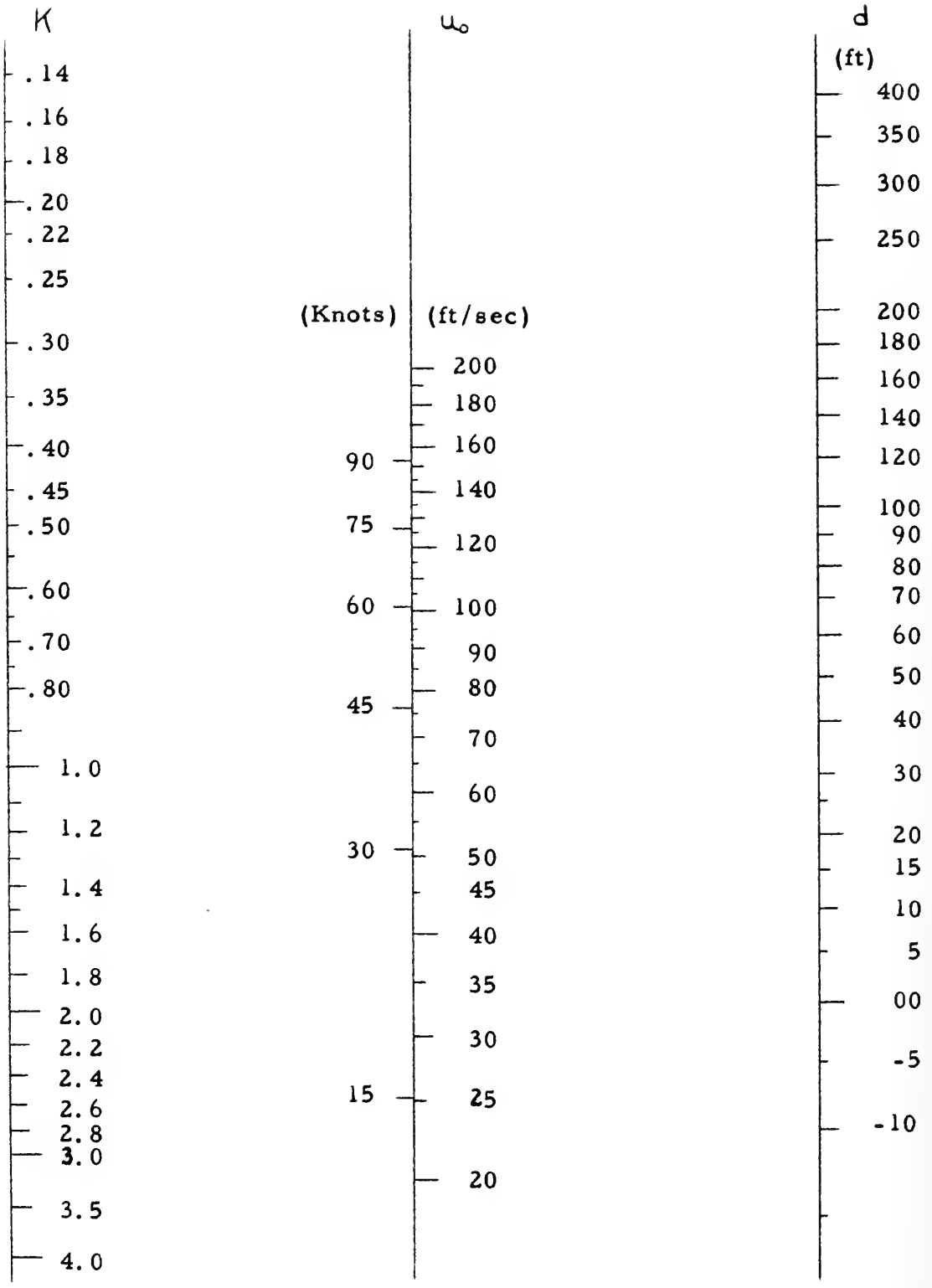

Figure 19. Nomograph relating the cavitation number K, free stream velocity u_o, and depth of operation d.

Thesis
S22 Savage
An analytical investigation of the ducted propeller for hydrodynamic propulsion.